

## Interstitial $Tl^0$ atoms in alkali halides: ESR study of a $\langle 111 \rangle$ -oriented $Tl_2^+$ center

S. V. Nistor,\* E. Goovaerts, B.-r. Yang,<sup>†</sup> and D. Schoemaker

*Physics Department, University of Antwerp (Universitaire Instelling Antwerpen), B-2610 Wilrijk, Belgium*

(Received 4 March 1983)

A  $\langle 111 \rangle$ -oriented  $Tl_2^+$  center is produced above 220 K by x-ray irradiation of  $Tl^+$ -doped KCl and RbCl. A careful analysis of the X-band electron-spin-resonance spectra establishes that the two Tl nuclei are equivalent, which implies that the center possesses inversion symmetry. The model proposed is a  $Tl_2^+$  center on a single cation site. Its production is believed to involve the trapping of a mobile anion vacancy between a distant pair of substitutional  $Tl^+$  impurities and the trapping of an electron in whatever order, an asymmetric relaxation of a  $Tl_2^+$  center towards a cation site and the diffusing away of a divacancy. In a formal sense this  $Tl_2^+$  center may be viewed as being an interstitial  $Tl^0$  atom trapped by a substitutional  $Tl^+$  impurity, although no mobile interstitial  $Tl^0$  as such is produced by the x-ray irradiation. Its structure is formally analogous to the interstitial halogen atom center, the  $H$  center. The possible effect of the presence of  $\langle 111 \rangle$ -oriented  $Tl_2^+$  on the lasing properties of  $Tl^0(1)$  centers is briefly discussed.

### I. INTRODUCTION

Several interesting thallium defects can be produced in  $Tl^+$ -doped alkali halides. X-ray irradiation at 77 K of, say, KCl: $Tl^+$  produces by simple electron trapping the so-called primary  $Tl^0(0)$  center,<sup>1-3</sup> i.e., a  $Tl^0(6p^1)$  atom occupying an unperturbed cation site. The remarkable thing about this center is that its electron-spin-resonance (ESR) spectrum has so far eluded detection and a possible reason for this has been proposed.<sup>4,5</sup>

X-ray irradiation above 220 K creates the following  $Tl^0$ -atom defects whose structures were established through a careful ESR analysis<sup>3,6</sup>: a substitutional  $Tl^0$ -atom center perturbed by a *single* nearest-neighbor anion vacancy, called the  $Tl^0(1)$  center, and one which is flanked by *two* such vacancies, the  $Tl^0(2)$  center. The notation is transparent. The current interest in the  $Tl^0(1)$  centers derives from the fact that they are superior lasing centers: Stable tunable near-infrared color-center lasers are constructed possessing high cw and picosecond pulse outputs which cover the (1.3–1.9)- $\mu$ m range in various alkali halides.<sup>7-10</sup>

Higher laser outputs are obtained with higher  $Tl^0(1)$  concentrations and this can be achieved through stronger  $Tl^+$  doping. However, the probability of having nearest-neighbor substitutional  $Tl^+$ - $Tl^+$  pairs increases concomitantly and these too can trap electrons creating a  $\langle 110 \rangle$ -oriented substitutional  $Tl_2^+$  dimer center.<sup>11</sup> This will be called the " $Tl_2^+(\langle 110 \rangle)$ " center from here on. Again its electronic structure was determined from ESR studies.<sup>12</sup> The  $Tl_2^+(\langle 110 \rangle)$  may interfere with the lasing properties of the crystals<sup>9</sup> but a large fraction of them can be eliminated by optical bleaching.

In this paper we present the ESR analysis of yet another thallium center that is produced above 220 K, in all crystals except the ones with very low  $Tl^+$  doping levels. It is in many respects the most unusual one of all the thallium defects. In Sec. III it will be shown that it is a  $\langle 111 \rangle$ -oriented  $Tl_2^+$  center, called  $Tl_2^+(\langle 111 \rangle)$ , possessing inversion symmetry. Its proposed model, a  $Tl_2^+$  molecule ion on a single cation site, is discussed in Sec. V together with

the possible production mechanisms. It is argued in Sec. VI that this  $Tl_2^+(\langle 111 \rangle)$  center represents the interstitial  $Tl^0$  center trapped by another  $Tl^+$  impurity, very much like the  $H$  center, a halogen  $X_2^-$  molecule on a single anion site, which is the manifestation of the interstitial halogen atom  $X^0$  center.<sup>13-15</sup> The final section ends with a brief discussion of the thermal decay mechanism and of the possible influence the  $Tl_2^+(\langle 111 \rangle)$  presence has on the  $Tl^0(1)$  center laser.<sup>7-10</sup>

### II. EXPERIMENTAL

The single crystals of  $Tl^+$ -doped KCl and RbCl were grown from the melt in silica ampoules by the Bridgman-Stockbarger technique from suprapure (Merck) KCl and RbCl to which 2 mol % of TlCl of ultrapure (Ventron) grade was added. Prior to growing, the material was purified from oxygen by processing it in a reactive atmosphere.<sup>16,6</sup> The  $Tl^+$  concentration in the crystals was determined from the height of its absorption band at 247 nm and was found to be  $\sim 0.2$  mol %. Several other KCl: $Tl^+$  samples with lower doping levels were also used for determining the dependence of the thallium centers on  $Tl^+$  concentration. The other experimental procedures are the same as in Ref. 3. In particular, the tungsten x-ray source was operated at 50 kV and 50 mA, and the white light excitations were performed with a 60-W halogen lamp.

### III. ANALYSIS OF THE $Tl_2^+(\langle 111 \rangle)$ ESR SPECTRA

#### A. Qualitative analysis

The ESR spectrum which we shall identify with a  $\langle 111 \rangle$ -oriented  $Tl_2^+$  molecule ion, henceforth called  $Tl_2^+(\langle 111 \rangle)$ , can be readily produced in KCl and RbCl doped with  $\sim 0.2$  mol % of TlCl by a x-ray irradiation above 220 K. The irradiation times are usually 30 min or more (see Sec. IV).

KCl possesses the narrowest lines (between 2.0 and 5.0 mT) and the ESR spectra taken at 13 K are presented in

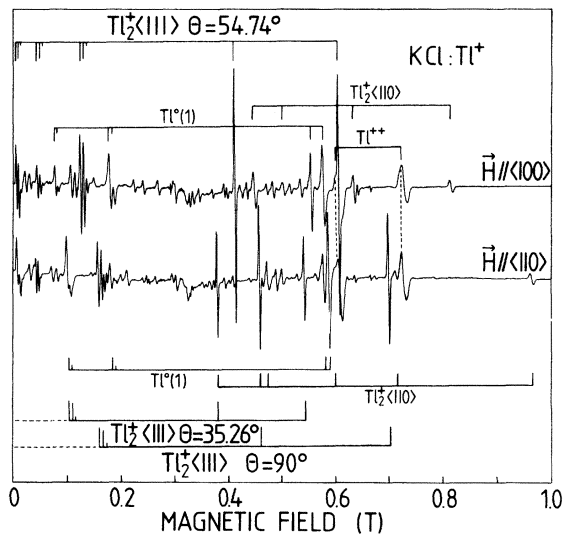


FIG. 1. ESR spectra at 13 K of the  $Tl_2^+(\langle 111 \rangle)$  center in KCl containing 0.2 mol % of TlCl for  $\vec{H} \parallel \langle 100 \rangle$  and  $\vec{H} \parallel \langle 110 \rangle$ . The microwave frequency is 9.23 GHz. The lines originating from  $Tl^0(1)$ ,  $Tl^{2+}$ , and  $Tl_2^+(\langle 110 \rangle)$  are also indicated. The sample had been x-ray irradiated for 30 min at room temperature and optically bleached with 460-nm light at 80 K in order to reduce  $Tl_2^+(\langle 110 \rangle)$ .

Fig. 1. The lines corresponding to the well-studied  $Tl^0(1)$ ,<sup>3</sup>  $Tl^{2+}$ ,<sup>1,17,18</sup> and the orthorhombic  $\langle 110 \rangle$ -oriented  $Tl_2^+$  dimer center<sup>12</sup> [called  $Tl_2^+(\langle 110 \rangle)$  from here on] have been indicated.  $Tl^0(1)$  possesses axial symmetry around  $\hat{z} \parallel \langle 001 \rangle$  and the  $Tl^{2+}$  line positions are isotropic.

An angular variation of the spectra reveals that there is an ESR pattern possessing axial symmetry around  $\hat{z} \parallel \langle 111 \rangle$ . These spectra exhibit many lines extending from zero field up to 700 mT and they are characterized by the angle  $\theta$  that the symmetry axis  $z$  makes with the external magnetic field  $\vec{H}$ .

It was established through a careful study of their production, thermal decay, microwave saturation behavior, and observability as a function of temperature, that all these lines belong to the same center.

The spectrum is complex and does not lend itself to a quick qualitative interpretation. However, the lines can be divided into a set of high-field lines (between 380 and 700 mT) and a set of low-field lines (below 165 mT). This is reminiscent of the ESR patterns of the  $\langle 110 \rangle$ -oriented

$Tl_2^+$  center which were analyzed recently.<sup>12</sup> We have confirmed that this ESR pattern of  $\langle 111 \rangle$  symmetry does indeed originate from a  $Tl_2^+$  species.

Thallium has two isotopes both with nuclear spin  $I = \frac{1}{2}$ ; the 70% abundant  $^{205}Tl$  [nuclear moment  $\mu_I = 1.6115\mu_N$  (nuclear magnetons)] and the 30% abundant  $^{203}Tl$  ( $\mu_I = 1.5960\mu_N$ ). A  $Tl_2^+$  center comprises three isotopic species, namely  $(^{205}Tl-^{205}Tl)^+$ ,  $(^{205}Tl-^{203}Tl)^+$ , and  $(^{203}Tl-^{203}Tl)^+$  with relative abundances 49:42:9. The latter ratios hold for the cases where the two thallium nuclei are equivalent with respect to the magnetic field  $\vec{H}$ . The set of high-field lines does not show such three line isotopic splitting, but the low-field lines definitely do and with relative intensities that accurately obey the 49:42:9 ratios for every angle  $\theta$ . This is an important observation. It shows that the two thallium nuclei are equivalent for all orientations of the magnetic field, or in other words that the  $Tl_2^+(\langle 111 \rangle)$  center possesses inversion symmetry. Because of the much larger linewidth (6.0–10.0 mT) the  $Tl_2^+(\langle 111 \rangle)$  isotopic splittings are not observable in RbCl.

### B. Spin-Hamiltonian fitting

A quantitative fit of the ESR lines to a  $S = \frac{1}{2}$ ,  $I_1 = I_2 = \frac{1}{2}$  axial spin Hamiltonian (usual notation),

$$\frac{\mathcal{H}}{g_0\mu_B} = \frac{1}{g_0} \vec{H} \cdot \vec{g} \cdot \vec{S} + \vec{S} \cdot \vec{A}(Tl) \cdot [\vec{I}_1 + \vec{I}_2], \quad (1)$$

fully confirms the  $Tl_2^+$  hypothesis. This fitting was performed carefully using a computer diagonalization of (1) together with a least-squares-fitting procedure.<sup>12</sup> First, a fitting was performed using only the high-field lines (300–700 mT) which are essentially average line positions of the  $(^{205}Tl-^{205}Tl)^+$  and  $(^{205}Tl-^{203}Tl)^+$  species. Then, using the known ratio of the two thallium isotope nuclear moments, the values for the  $\vec{A}(^{205}Tl)$  and  $\vec{A}(^{203}Tl)$  components were derived and these were subsequently used and further refined in fitting the low-field lines.

Table I gives the values of the spin-Hamiltonian parameters for the dominant  $(^{205}Tl-^{205}Tl)$  center and Tables II and III, where for KCl the calculated and experimental line positions are compared, gives an idea of the excellent quality of the fit. Equally excellent fits were obtained for all the spectra in RbCl. Particularly satisfying is that the calculated isotopic splittings (IS) between  $(^{205}Tl-^{205}Tl)^+$  and  $(^{205}Tl-^{203}Tl)^+$  never exceed 25% of the linewidth of the high-field lines, thus proving that these splittings are indeed unobservable (Table II). In contrast, the observed

TABLE I. Spin-Hamiltonian parameters of the  $^{205}Tl_2^+(\langle 111 \rangle)$  center in  $Tl^+$ -doped KCl and RbCl. The hyperfine parameters and the linewidth  $\Delta H$  (between points of maximum slope) are given in mT. The signs of the hf parameters were established in Ref. 12.

Crystal	Temp. (K)	$g_{\parallel}^a$ $\langle 111 \rangle$	$g_{\perp}^a$	$A_{\parallel}(^{205}Tl)^b$ $\langle 111 \rangle$	$A_{\perp}(^{205}Tl)^b$	$\Delta H$
KCl	13	1.8668	1.4385	+ 188.0	-220.8	3.5±1.5
KCl	65	1.8648	1.4334	+ 187.7	-221.4	3.5±1.5
RbCl	13	1.8720	1.4264	+ 188.9	-210.6	8.0±2.0

<sup>a</sup>±0.0003

<sup>b</sup>±0.2 mT.

TABLE II. Comparison between the experimental ( $H_{\text{expt}}$ ) and calculated ( $H_{\text{calc}}$ ) ESR line positions of the high-field lines of the  $\text{Ti}_2^+(\langle 111 \rangle)$  center in  $\text{KCl}:\text{Ti}^+$  at 65 K. For these lines the isotopic splittings ( $\text{IS})_{\text{calc}}$  are not resolved. Also included are the experimental linewidth,  $\Delta H_{\text{expt}}$ , and the calculated unnormalized transition probability,  $P$ . The parameters of Table I were used. All units are mT except  $P$ .

	$\theta=35.26^\circ$	$\theta=35.26^\circ$	$\theta=54.74^\circ$	$\theta=54.74^\circ$	$\theta=90^\circ$	$\theta=90^\circ$
$H_{\text{expt}}$	380.4	541.6	414.5	607.5	459.9	701.9
$H_{\text{calc}}$	380.4	541.6	414.6	607.5	459.9	701.9
$\Delta H_{\text{expt}}$	2.5	2.0	5.0	3.0	2.0	
$(\text{IS})_{\text{calc}}$	0.00	0.54	0.01	0.68	0.01	0.91
$P$	0.94	0.81	0.46	0.47	0.46	0.42

isotopic splittings of the low-field lines are quite accurately reproduced (Table III). From which transitions between the levels of (1) the ESR lines originate is illustrated for  $\theta=54.74^\circ$  in Fig. 2. It should further be remarked that we could not accurately measure line positions below 70 mT and no attempt was made to make the correlation between experimental and calculated lines in this field region. However, the excellent fit obtained for the positions between 99 and 165 mT both for  $\text{KCl}$  and  $\text{RbCl}$  leaves no doubt about the correctness of the  $\text{Ti}_2^+$  interpretation.

### C. Discussion of the $g$ and $A$ components

The ESR parameters of  $\text{Ti}_2^+(\langle 111 \rangle)$  as given in Table I are very similar to those of  $\text{Ti}_2^+(\langle 110 \rangle)$  as determined in Ref. 12. Approximating for simplicity of comparison to axial symmetry the  $\text{Ti}_2^+(\langle 110 \rangle)$  parameters are

$$g_{\parallel} = 1.7618, \quad g_{\perp} = 1.2046, \quad (2)$$

and

$$A_{\parallel} = +190.4 \text{ mT}, \quad A_{\perp} = -258.4 \text{ mT}. \quad (3)$$

It was noted that  $\text{Ti}_2^+$  and the  $X_2^-$  centers<sup>19</sup> ( $X=\text{F,Cl,Br,I}$ ) possessed complementary electronic configurations and this permitted an analysis of the ESR parameters and a determination of the  $\text{Ti}_2^+$  electronic structure.<sup>12</sup>

A similar analysis can be applied to the  $\text{Ti}_2^+(\langle 111 \rangle)$  data. Comparing the  $\text{Ti}_2^+(\langle 111 \rangle)$  shifts  $\Delta g_i = g_0 - g_i$  in Table I with those of  $\text{Ti}_2^+(\langle 110 \rangle)$  in (2) one notices that the latter are larger. In fact one finds  $\lambda/E \cong 0.45$  for  $\text{Ti}_2^+(\langle 110 \rangle)$  (Ref. 12) and  $\lambda/E \cong 0.34$  for  $\text{Ti}_2^+(\langle 111 \rangle)$  where  $\lambda \approx 4900 \text{ cm}^{-1}$  is the  $\text{Ti}_2^+$  spin-orbit coupling constant and  $E$  the energy difference between the  $^2\Sigma_g$  ground state and the  $^2\Pi_g$  excited state. One concludes more generally that the  $\text{Ti}_2^+(\langle 111 \rangle)$  optical transitions should be

found at distinctly higher energies compared to those of  $\text{Ti}_2^+(\langle 110 \rangle)$ . In particular, the  $^2\Sigma_g \rightarrow ^2\Pi_u$  ( $^2A_{1g} \rightarrow ^2B_{2u}$ ) transition which occurs at  $1.76 \mu\text{m}$  for  $\text{Ti}_2^+(\langle 110 \rangle)$  should be shifted towards shorter wavelengths for  $\text{Ti}_2^+(\langle 111 \rangle)$ . If one scales this transition according to the two  $\lambda/E$  ratios obtained above, the absorption band should be found around  $1.3 \mu\text{m}$  for  $\text{Ti}_2^+(\langle 111 \rangle)$  in  $\text{KCl}$ . If so, this could interfere with the lasing properties of the  $\text{Ti}^0(1)$  center whose pumping transition is at  $1.05 \mu\text{m}$  and whose emission is positioned at  $1.5 \mu\text{m}$ .<sup>7,8</sup> A preliminary optical absorption experiment did not reveal a detectable absorption band near  $1.3 \mu\text{m}$ . There is one at  $845 \text{ nm}$  whose properties seem to coincide with those of  $\text{Ti}_2^+(\langle 111 \rangle)$ , but a definite correlation has not been established.

An analysis of the  $\text{Ti}_2^+(\langle 110 \rangle)$  hyperfine components (3) yields

$$\rho \cong 46 \text{ mT} \quad (4)$$

for the anisotropic part and

$$A_{\sigma} \cong -19 \text{ mT} \quad (5)$$

for the isotropic part of the hyperfine interaction. Of these recalculated and improved numbers  $\rho$  is identical to the one obtained in Ref. 12, but  $A_{\sigma}$  is somewhat smaller.

It was shown<sup>12</sup> that the  $A_{\sigma}$  value was the sum of two contributions namely  $-36 \text{ mT}$  originating from exchange polarization effects and  $+17 \text{ mT}$  from  $s$  mixing in the  $^2\Sigma_g$  ground state. A similar analysis yields for  $\text{Ti}_2^+(\langle 111 \rangle)$  the following results:

$$\rho \cong 52 \text{ mT} \quad (6)$$

which is comparable to the  $\text{Ti}_2^+(\langle 110 \rangle)$  value in (4) and

$$A_{\sigma} \cong -10 \text{ mT} \quad (7)$$

TABLE III. Comparison between the experimental ( $H_{\text{expt}}$ ) and calculated ( $H_{\text{calc}}$ ) ESR line positions of some measured low-field lines of the  $\text{Ti}_2^+(\langle 111 \rangle)$  center in  $\text{KCl}:\text{Ti}^+$  at 65 K. For these lines the isotopic splittings between the three possible  $\text{Ti}_2^+$  species are resolved because the linewidth  $\Delta H$  is about 2.7 mT. The parameters of Table I were used. All units are mT except the calculated unnormalized transition probability  $P$ .

	$\theta=35.26^\circ$		$\theta=54.74^\circ$		$\theta=90^\circ$	
	$(^{205}\text{Ti}-^{205}\text{Ti})^+$	$(^{205}\text{Ti}-^{203}\text{Ti})^+$	$(^{205}\text{Ti}-^{205}\text{Ti})^+$	$(^{205}\text{Ti}-^{203}\text{Ti})^+$	$(^{205}\text{Ti}-^{205}\text{Ti})^+$	$(^{205}\text{Ti}-^{203}\text{Ti})^+$
$H_{\text{expt}}$	104.7	99.0	132.5	126.4	163.9	157.5
$H_{\text{calc}}$	104.7	99.1	132.1	126.1	164.3	157.9
$P$	0.34	0.35	0.15	0.15	0.25	0.25

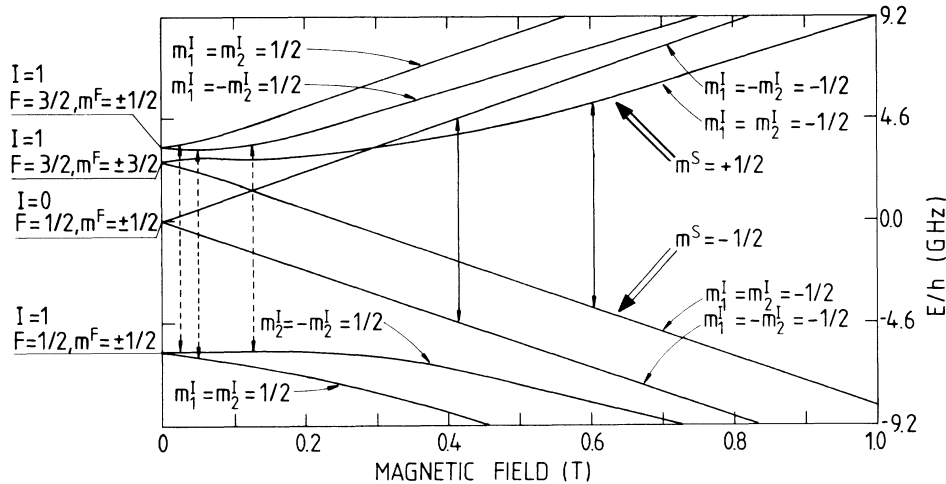


FIG. 2. Energy-level scheme for  $\theta=54.74^\circ$ , and corresponding to  $(^{205}\text{Tl}-^{205}\text{Tl})^+$  of the  $\text{Tl}_2^+(\langle 111 \rangle)$  center ground state in  $\text{KCl:Tl}^+$ . All transitions indicated were observed at X band but the ones below  $\sim 100$  mT could not be accurately measured. For the low-field lines ( $< 165$  mT) the Tl isotope effects are resolved (see Fig. 1 and Table III). The quantum number  $F$  corresponds to  $\vec{F}=\vec{S}+\vec{I}$ .

which is larger than the  $\text{Tl}_2^+(\langle 110 \rangle)$  value in (5). This change is attributed to an *increased*  $s$  mixing in the  $\text{Tl}_2^+(\langle 111 \rangle)$  ground state compared to  $\text{Tl}_2^+(\langle 110 \rangle)$ . The significance of these results will be further discussed in Sec. VI.

#### IV. SOME PRODUCTION, THERMAL AND OPTICAL PROPERTIES

##### A. Production at room temperature

In KCl and RbCl samples containing  $\sim 0.2$  mol % of  $\text{Tl}^+$ , the  $\text{Tl}_2^+(\langle 111 \rangle)$  center can be produced directly by x-ray irradiation above 220 K, room temperature in particular. Because it is well established<sup>3,20-22</sup> that anion vacancies produced by the x-ray irradiation become mobile above 220 K this observation implies that an anion vacan-

cy is either involved in the  $\text{Tl}_2^+(\langle 111 \rangle)$  structure and/or that it is necessary for its production (see Sec. V). The production of  $\text{Tl}_2^+(\langle 110 \rangle)$ ,  $\text{Tl}^0(1)$ , and  $\text{Tl}_2^+(\langle 111 \rangle)$  as a function of irradiation time at 300 K is given in Fig. 3.

The intensities have been normalized to the value obtained after 120 min of irradiation. It is seen that  $\text{Tl}_2^+(\langle 110 \rangle)$ , which is a simple trapped electron center, reaches most of its final intensity during the first 10 min and after 20–30 min it exhibits already a definite decay.  $\text{Tl}_2^+(\langle 111 \rangle)$  and  $\text{Tl}^0(1)$  acquire a large fraction of their intensity only after 30 min and keep on increasing slowly afterwards. The  $\text{Tl}_2^+(\langle 111 \rangle)$  production is somewhat faster than the  $\text{Tl}^0(1)$  one.

##### B. X-ray irradiation at 77 K followed by a warm up

In crystals containing a lower  $\text{Tl}^+$  concentration ( $\sim 0.02$  mol %) another procedure is possible: X-ray irradiation at 77 K followed by a warm up to above 220 K also produces  $\text{Tl}_2^+(\langle 111 \rangle)$  together with  $\text{Tl}^0(1)$ . This is illustrated in Fig. 4 where the results of a pulse anneal above 210 K are presented. At the latter temperature the  $V_K$  center<sup>19</sup> (the self-trapped hole center) has already decayed destroying in the process some primary  $\text{Tl}^0(0)$  and  $\text{Tl}_2^+(\langle 110 \rangle)$  and producing a large amount of  $\text{Tl}^{2+}$ . The relative intensities in Fig. 4 are completely arbitrary.

It is seen from Fig. 4 that  $\text{Tl}_2^+(\langle 111 \rangle)$  and  $\text{Tl}^0(1)$  are produced simultaneously above 220 K. This again strongly supports the conclusion (Sec. IV A) that an anion vacancy is involved in the structure of the  $\text{Tl}_2^+(\langle 111 \rangle)$  center or that it is an indispensable entity in the production of  $\text{Tl}_2^+(\langle 111 \rangle)$  (see Sec. V). In the (260–300)-K region  $\text{Tl}^0(1)$  decays but  $\text{Tl}_2^+(\langle 110 \rangle)$  and  $\text{Tl}_2^+(\langle 111 \rangle)$  keep on increasing. In this region the primary  $\text{Tl}^0(0)$  centers, which are unobservable in ESR, are known to decay. The mobile electrons thus produced are trapped by nearest-neighbor  $\text{Tl}^+-\text{Tl}^+$  pairs enhancing the  $\text{Tl}_2^+(\langle 110 \rangle)$  concentration but they destroy part of the  $\text{Tl}^0(1)$  centers. In the same temperature region  $\text{Tl}_2^+(\langle 111 \rangle)$  increases fur-

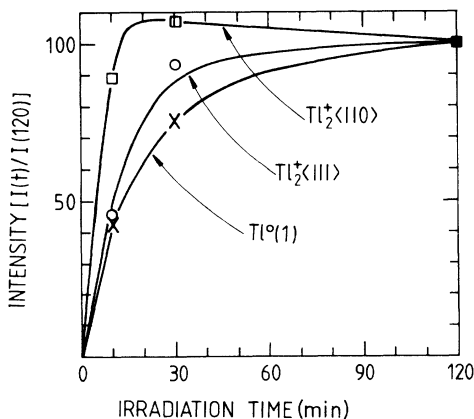


FIG. 3. Production by x-ray irradiation at 300 K of the  $\text{Tl}_2^+(\langle 111 \rangle)$ ,  $\text{Tl}^0(1)$ , and  $\text{Tl}_2^+(\langle 110 \rangle)$  centers as a function of time in KCl containing  $\sim 0.2$  mol % of  $\text{TlCl}$ . The curves have been normalized to the 120-min value.

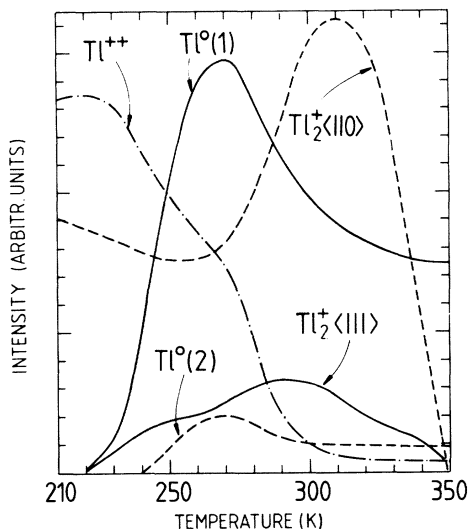


FIG. 4. Pulse anneal above 210 K of a  $KCl:Tl^+$  sample ( $\sim 0.02$  mol %) which had first been x-ray irradiated at 77 K for 20 min. At 210 K the  $Cl_2^- V_K$  centers have decayed producing  $Tl^{2+}$  and destroying some  $Tl_2^+$  and primary  $Tl^0(0)$  in the process.

ther. Both  $Tl_2^+(\langle 111 \rangle)$  and  $Tl_2^+(\langle 110 \rangle)$  decay from 300 K onwards and their half-life at this temperature is roughly 1 h but  $Tl_2^+(\langle 111 \rangle)$  decays somewhat faster than  $Tl_2^+(\langle 110 \rangle)$ . At 350 K they have disappeared completely. The  $Tl^0(1)$  centers remain stable until<sup>3</sup> 410 K.

#### C. Production as a function of $Tl^+$ concentration

The production of  $Tl_2^+(\langle 110 \rangle)$ ,  $Tl_2^+(\langle 111 \rangle)$ , and  $Tl^0(1)$  as a function of  $Tl^+$  concentration can be described as follows. The  $Tl_2^+(\langle 110 \rangle)$  rises fast, close to quadratically, with the  $Tl^+$  content.  $Tl_2^+(\langle 111 \rangle)$  and  $Tl^0(1)$ , on the other hand, also increase with  $Tl^+$  concentration, but tend to level off above 0.05 mol % of  $Tl^+$ . It is noteworthy that hardly any  $Tl^0(2)$  centers are produced in the heavily  $Tl^+$ -doped crystals, an observation that was not stressed in Ref. 3 (see Sec. VI).

#### D. Thermal decay and optical excitation

A few experiments were performed in order to obtain insight into the thermal decay mechanism of the  $Tl_2^+(\langle 111 \rangle)$  center. In a first experiment a sample was x-ray irradiated for 30 min at room temperature and was then subjected at low temperatures ( $< 180$  K) to a few minutes of white light excitation. The white light mainly excites the  $Tl_2^+(\langle 110 \rangle)$  absorption bands at<sup>11,12</sup> 460, 860, and 1760 nm and the  $F$  center at 540 nm producing mobile electrons in both cases. The  $Tl_2^+(\langle 110 \rangle)$  and  $Tl^{2+}$  are observed to decrease strongly by this treatment but the  $Tl^0(1)$  and  $Tl_2^+(\langle 111 \rangle)$  increase substantially. This technique was used to obtain cleaner  $Tl_2^+(\langle 111 \rangle)$  ESR spectra. Figure 1 represents an intermediate step with a certain amount of  $Tl_2^+(\langle 110 \rangle)$  left for orientation and reference purposes.

The same experiment was repeated but now on a sample which had been x-ray irradiated at 260 K, i.e., a tempera-

ture at which  $Tl_2^+(\langle 111 \rangle)$  possesses no thermal decay (Fig. 4). Again  $Tl_2^+(\langle 110 \rangle)$  and  $Tl^{2+}$  are destroyed and  $Tl^0(1)$  is enhanced but  $Tl_2^+(\langle 111 \rangle)$  now shows hardly any increase.

In another experiment a sample was x-ray irradiated at room temperature and  $Tl_2^+(\langle 111 \rangle)$  and  $Tl_2^+(\langle 110 \rangle)$  were allowed to decay at that temperature for about 2 h. Typically about 25% of  $Tl_2^+(\langle 111 \rangle)$  was left and about 35% of  $Tl_2^+(\langle 110 \rangle)$ . A subsequent white light excitation at 180 K (where anion vacancies are immobile) destroys the remaining  $Tl_2^+(\langle 110 \rangle)$  within 1 min but  $Tl_2^+(\langle 111 \rangle)$  almost doubles in intensity within the first 30 sec after which it remains constant.

Finally, if a sample containing  $Tl_2^+(\langle 111 \rangle)$  is warmed to 350 K for a few minutes all  $Tl_2^+(\langle 111 \rangle)$  disappears and its concentration cannot be regenerated by a white light excitation below 180 K. The implications of these observations for the thermal decay of  $Tl_2^+(\langle 111 \rangle)$  will be discussed in Sec. VI.

### V. MODEL FOR THE $Tl_2^+(\langle 111 \rangle)$ CENTER AND PRODUCTION MECHANISM

The model that will be proposed for the  $Tl_2^+(\langle 111 \rangle)$  center must account for two crucial observations: (i) the  $Tl_2^+(\langle 111 \rangle)$  center possesses inversion symmetry (Sec. III) and (ii) a negative ion vacancy is either involved in the structure or it is essential in its production mechanism (Secs. IV A and IV B).

#### A. The trivacancy model

In trying to find a  $\langle 111 \rangle$ -oriented  $Tl_2^+$  one starts from the observation [Fig. 5(a)] that moving away from a substitutional  $Tl^+$  impurity at (0,0,0) the nearest possible substitutional  $Tl^+$  along  $\langle 111 \rangle$  is encountered at  $(2a, 2a, 2a)$

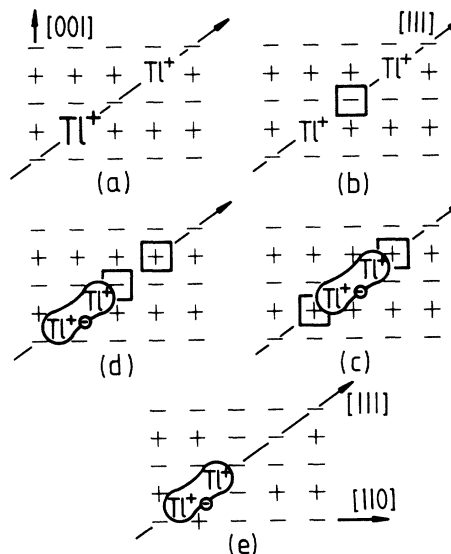


FIG. 5. Schematic production sequence presented in a  $(110)$  plane of the  $Tl_2^+(\langle 111 \rangle)$  center by x-ray irradiation at 240 K. This production sequence is based on a  $\langle 111 \rangle$ -oriented distant pair of substitutional  $Tl^+$  ions in an alkali-halide lattice but other pairs also contribute (see Fig. 6).

where  $a$  is the smallest halogen-alkali distance. In between sits a  $\text{Cl}^-$  at  $(a, a, a)$ . A mobile negative ion vacancy produced by the x-ray irradiation above 220 K can be stabilized at  $(a, a, a)$  in between the two  $\text{Tl}^+$  impurities [Fig. 5(b)]. This  $\langle 111 \rangle$ -oriented  $\text{Tl}^+$ -anion-vacancy- $\text{Tl}^+$  complex can now trap an electron. It could be trapped by either one of the  $\text{Tl}^+$  to form a  $\text{Tl}^0$  atom, but the center can lower its energy by forming a molecular bond between  $\text{Tl}^0$  and  $\text{Tl}^+$  thus producing a  $\langle 111 \rangle$ -oriented  $\text{Tl}_2^+$ . One can envisage the two thalliums relaxing symmetrically towards each other resulting in a  $\text{Tl}_2^+$  whose midpoint is positioned exactly at the anion site [Fig. 5(c)]. Such a model possesses inversion symmetry but it is a most awkward one: A positive molecule ion is situated at a negative ion site.

### B. The single-vacancy model

The trivacancy model of Fig. 5(c) as discussed in the foregoing paragraph (Sec. V A) can hardly be taken seriously. Therefore, we propose the following: Rather than relaxing symmetrically towards the anion vacancy, the two thalliums relax to one of the two symmetrically positioned cation sites [Fig. 5(d)]. However, in such a model the  $\langle 111 \rangle$ -oriented  $\text{Tl}_2^+$  would be perturbed on one side by a divacancy and the  $\text{Tl}_2^+(\langle 111 \rangle)$  center would not possess inversion symmetry and consequently no equivalent Tl nuclei. The final step then is to propose that the  $\langle 111 \rangle$ -oriented divacancy diffuses away either as a unit or as separate vacancies [Fig. 5(e)]. Such diffusion is possible because both the anion vacancy<sup>3,20-22</sup> and the cation vacancy<sup>23</sup> are independently mobile above 220 K.

### C. Alternative production schemes

Accepting the model for the  $\text{Tl}_2^+(\langle 111 \rangle)$  center as in Fig. 5(e) one realizes that there are at least three other pairs of substitutional  $\text{Tl}^+$  ions from which the  $\text{Tl}_2^+(\langle 111 \rangle)$  center can be produced using essentially the same production sequence as in Figs. 5(a)–5(e). The configurations are given in Figs. 6(a)–6(c). Inspection shows that these pairs can trap an anion vacancy in between or next to them. Subsequent trapping of an electron, an

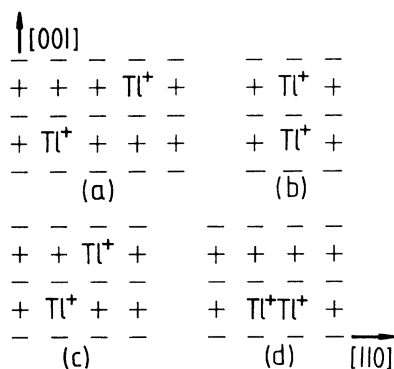


FIG. 6. Various pairs of  $\text{Tl}^+$  ions in an alkali halide which can trap an anion vacancy in between or next to them and which can all result in a  $\text{Tl}_2^+(\langle 111 \rangle)$  center [Fig. 7(a)] after asymmetric relaxation of the  $\text{Tl}_2^+$  molecule ion.

asymmetric relaxation of the  $\text{Tl}_2^+$  towards a cation vacancy, the diffusing away of a divacancy, and finally the seeking out of the  $\langle 111 \rangle$  equilibrium orientation leaves one with identically the same  $\text{Tl}_2^+(\langle 111 \rangle)$  model as in Fig. 5(e). It is quite possible and even likely that all these pairs contribute to the formation of  $\text{Tl}_2^+(\langle 111 \rangle)$  centers. This explains why this rather unusual center is produced rapidly and with concentrations that are comparable to the  $\text{Tl}^0(1)$  one. Furthermore, because these  $\text{Tl}^+$  pairs compete strongly with the isolated  $\text{Tl}^+$  impurities for mobile anion vacancies it is also clear why very few  $\text{Tl}^0(2)$  centers<sup>3</sup> are produced in the heavily doped crystals. Indeed, the production of  $\text{Tl}^0(2)$  requires two anion vacancies.

## VI. DISCUSSION AND CONCLUSIONS

The model proposed in Fig. 5(e) and Fig. 7(a) for the  $\text{Tl}_2^+(\langle 111 \rangle)$  center, i.e., a  $\text{Tl}_2^+$  occupying a single cation site, is the most simple and the most probable one. The  $\text{Tl}_2^+(\langle 111 \rangle)$  is a rather unusual center: It may be considered to be an interstitial  $\text{Tl}^0$  atom trapped by a substitutional  $\text{Tl}^+$  impurity although it is believed by inference from the discussion in Sec. V that no  $\text{Tl}^0$  interstitials are directly produced by the x-ray irradiation. The oblong  $\text{Tl}_2^+$  has more room in a  $\langle 111 \rangle$  direction and this is precisely the direction of the  $\text{F}_2^- H$  center in LiF.<sup>15</sup> The  $H$  center is the interstitial halogen atom,  $X^0$ , center and it

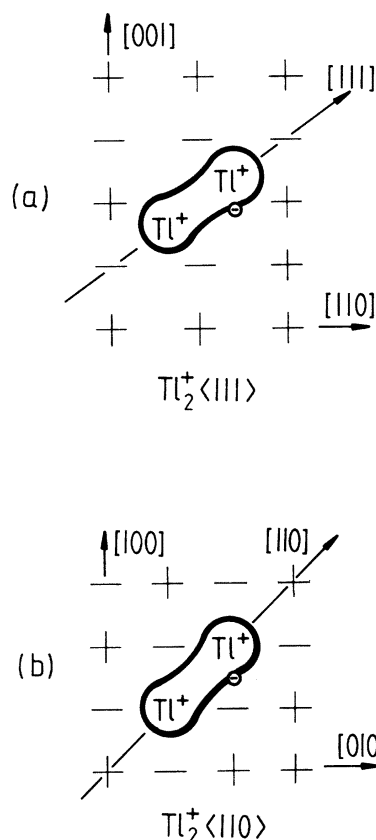


FIG. 7. (a) Schematic model of the  $\text{Tl}_2^+(\langle 111 \rangle)$  center in an alkali-halide lattice presented in a  $(110)$  plane; (b) schematic model of the  $\text{Tl}_2^+(\langle 111 \rangle)$  center presented in a  $(100)$  plane.

manifests itself as a  $X_2^-$  molecule ion occupying a *single* anion site. This is in contrast to the  $V_K$  center<sup>19</sup> where the  $X_2^-$  occupies *two* anion sites. The fact that in KCl and KBr the  $H$  center is  $\langle 110 \rangle$  oriented<sup>13,14</sup> is merely a consequence of the forming of two additional weak bonds of the  $\text{Cl}_2^-$  and  $\text{Br}_2^-$  with the two halogen ions flanking them. Inasmuch that the  $\text{Tl}_2^+(\langle 110 \rangle)$  center in Fig. 7(b) may be considered to be the trapped electron analog (be it with impurity ions) of the  $V_K$  center, the  $\text{Tl}_2^+(\langle 111 \rangle)$  center in Fig. 7(a) may be viewed as the corresponding  $H$ -center analog.

This parallelism between  $\text{Tl}_2^+(\langle 110 \rangle)$  and  $\text{Tl}_2^+(\langle 111 \rangle)$  on the one hand and the  $V_K$  center and the  $H$  center on the other hand is also reflected in the behavior of the  $g$  and hyperfine components. For instance, the  $g$  shift of the  $\text{Cl}_2^- H$  center in KCl (Ref. 24) is considerably smaller than the  $\text{Cl}_2^- V_K$ -center shift<sup>19</sup> ( $g_1 = 2.0224$  vs  $g_1 = 2.0435$ ), in agreement with the observation that the  $H$ -center optical absorption bands are at higher energies<sup>14</sup> (3.70 eV) than those of the  $V_K$  center<sup>25</sup> (3.40 eV). The  $g$  shifts of  $\text{Tl}_2^+(\langle 110 \rangle)$  and  $\text{Tl}_2^+(\langle 111 \rangle)$  exhibit a similar trend (see Sec. III C).

The  $\text{Cl}_2^- H$ -center hyperfine components<sup>24</sup> are distinctly larger than the  $\text{Cl}_2^- V_K$ -center components.<sup>19</sup> This behavior seems opposite to the observed reduction in going from  $\text{Tl}_2^+(\langle 110 \rangle)$  to  $\text{Tl}_2^+(\langle 111 \rangle)$ , but in fact the basic behavior is the same: The anisotropic part of the  $\text{Cl}_2^-$  hyperfine interaction is virtually the same for the  $V_K$  center<sup>19</sup> [ $\rho(\text{Cl}) = 3.23$  mT] as for the  $H$  center<sup>26</sup> [ $\rho(\text{Cl}) = 3.22$  mT] but the corresponding isotropic parts increase from<sup>19</sup>  $A_\sigma(\text{Cl}) = 3.91$  mT for  $V_K$  to<sup>26</sup> 4.54 mT for  $H$ . Similarly, the isotropic part increases from<sup>12</sup>  $A_\sigma(\text{Tl}) = -19$  mT for  $\text{Tl}_2^+(\langle 110 \rangle)$  to  $A_\sigma(\text{Tl}) = -10$  mT for  $\text{Tl}_2^+(\langle 111 \rangle)$  (see Sec. III C). For both the  $X_2^-$  and  $\text{Tl}_2^+$  centers this change is caused by an increase in  $s$  mixing in the  $s$ - $p$  hybrids of the ground state  $\sigma$ -type wave function. Such an increase in  $s$  mixing and excited state energies was attributed to a small reduction in the  $\text{Cl}_2^- H$ -center internuclear distance compared to the  $V_K$ -center one. Similarly one concludes that there is a small reduction in the  $\text{Tl}_2^+(\langle 111 \rangle)$  internuclear distance compared to  $\text{Tl}_2^+(\langle 110 \rangle)$ . Such a behavior adds support to the proposed  $\text{Tl}_2^+(\langle 111 \rangle)$  model in Fig. 7(a) where the  $\text{Tl}_2^+$  is indeed more squeezed than in the  $\text{Tl}_2^+(\langle 110 \rangle)$  model of Fig. 7(b).

In contrast to the  $H$  center which starts to reorient<sup>14,27</sup> at very low temperatures (10.5 K) the  $\text{Tl}_2^+(\langle 111 \rangle)$  center exhibits no detectable motional properties. No line

broadening is observed as the temperature is raised and  $\text{Tl}_2^+$  remains observable up to 140 K, whereas for the  $H$  center in KCl the ESR lines start to broaden at 29 K reflecting<sup>28</sup> the very rapid reorientation of the  $\text{Cl}_2^-$  molecule ion.

From the observations presented in Sec. IVD one can construct the following thermal decay mechanism for  $\text{Tl}_2^+(\langle 111 \rangle)$ . The first step in the decay above 300 K is the freeing of an electron leaving two  $\text{Tl}^+$  ions on a single cation site. This center, which we shall call  $\text{Tl}_2^{2+}$ , subsequently decays with a somewhat slower rate compared to the electron release process. Probably a  $\text{Tl}^+$  breaks away from the  $\text{Tl}_2^{2+}$  center and moves interstitially before it is trapped somewhere. However, some  $\text{Tl}_2^{2+}$  evidently remain because the  $\text{Tl}_2^+(\langle 111 \rangle)$  concentration can be partly regenerated by a white light excitation of the sample at temperatures below 180 K, i.e., the temperature region where anion vacancies are immobile. The electrons generated by the optical excitation are strongly attracted by the remaining positively charged  $\text{Tl}_2^{2+}$  reforming  $\text{Tl}_2^+(\langle 111 \rangle)$  centers. Such regeneration is impossible after warm up to 350 K implying that such treatment destroys all  $\text{Tl}_2^{2+}$ .

This leads us finally to a point of possible practical importance. It was suggested in Sec. VC that the  $\text{Tl}_2^+(\langle 111 \rangle)$  center could possess an optical absorption band in the 1.3- $\mu\text{m}$  region although in a preliminary experiment no absorption was detected there. Nevertheless if one would be worried about the possible influence of the  $\text{Tl}_2^+(\langle 111 \rangle)$  presence on the  $\text{Tl}^0(1)$  center laser<sup>7,8</sup> performance at 1.5  $\mu\text{m}$  one may get rid of the  $\text{Tl}_2^+(\langle 111 \rangle)$  [and of the  $\text{Tl}_2^+(\langle 110 \rangle)$ ] by a warm up to 350 K for a few minutes. This procedure does not affect the remaining  $\text{Tl}^0(1)$  centers because they are stable up to<sup>3</sup> 410 K.

#### ACKNOWLEDGMENTS

It is a pleasure to thank I. Ursu for his kind and continuous cooperation, A. Bouwen for his experimental assistance, and the Secretariaat Generaal van de Internationale Culturele Betrekkingen (Vlaamse Gemeenschap) for support for S. V. Nistor while at the University of Antwerp. One of us (B.-r. Yang) is indebted to the Universitaire Instelling Antwerpen for a scholarship. Financial support from the I.I.K.W. (Interuniversitair Instituut voor Kernwetenschappen) and the Geconcerteerde Acties is gratefully acknowledged.

\*Permanent address: Central Institute of Physics, I.F.T.M., C.P.MG-7, R-76900 Magurele-Bucuresti, Rumania.

†Permanent address: Department of Physics, Beijing University, Beijing, China.

<sup>1</sup>C. J. Delbecq, A. K. Ghosh, and P. H. Yuster, *Phys. Rev.* **151**, 599 (1966); **154**, 797 (1967).

<sup>2</sup>W. B. Hadley, S. Pollock, R. G. Kaufman, and H. N. Hersh, *J. Chem. Phys.* **45**, 2040 (1966).

<sup>3</sup>E. Goovaerts, J. Andriessen, S. V. Nistor, and D. Schoemaker, *Phys. Rev. B* **24**, 29 (1981).

<sup>4</sup>W. Van Puymbroeck, J. Andriessen, and D. Schoemaker, *Phys.*

*Rev. B* **24**, 2412 (1981).

<sup>5</sup>W. Van Puymbroeck, D. Schoemaker, and J. Andriessen, *Phys. Rev. B* **26**, 1139 (1982).

<sup>6</sup>S. V. Nistor, E. Goovaerts, A. Bouwen, and D. Schoemaker, *Phys. Rev. B* **27**, 5797 (1983).

<sup>7</sup>W. Gellerman, F. Lüty, and C. R. Pollock, *Opt. Commun.* **39**, 391 (1981).

<sup>8</sup>L. F. Mollenauer, N. D. Viera, and L. Szeto, *Opt. Lett.* **9**, 414 (1982).

<sup>9</sup>L. F. Mollenauer, N. D. Viera, and L. Szeto, *Phys. Rev. B* **27**, 5332 (1983).

- <sup>10</sup>F. J. Ahlers, F. Lohse, J. M. Spaeth, and L. Mollenauer, *Phys. Rev. B* **27**, 1249 (1983).
- <sup>11</sup>C. J. Delbecq, E. Hutchinson, and P. H. Yuster, *J. Phys. Soc. Jpn.* **36**, 913 (1974).
- <sup>12</sup>B.-r. Yang, E. Goovaerts, and D. Schoemaker, *Phys. Rev. B* **27**, 1507 (1983). Because of an error in the calibration procedure the  $Tl^+$  concentrations given in this paper are too low; they should be multiplied by a factor of 10–15.
- <sup>13</sup>W. Känzig and T. O. Woodruff, *J. Phys. Chem. Solids* **9**, 70 (1958).
- <sup>14</sup>C. J. Delbecq, J. L. Kolopus, E. L. Yasaitis, and P. H. Yuster, *Phys. Rev.* **154**, 866 (1967).
- <sup>15</sup>Y. H. Chu and R. L. Mieher, *Phys. Rev.* **188**, 1311 (1969).
- <sup>16</sup>I. Ursu, S. V. Nistor, M. Voda, L. C. Nistor, and V. Teodorescu, Central Institute for Physics (Bucharest-Magurele) Report No. LOP-30-1982 (unpublished).
- <sup>17</sup>W. Dreybrodt and D. Silber, *Phys. Status Solidi* **20**, 337 (1967).
- <sup>18</sup>W. Frey, R. Huss, H. Seidel, and E. Werkmann, *Phys. Status Solidi B* **68**, 257 (1975).
- <sup>19</sup>D. Schoemaker, *Phys. Rev. B* **7**, 786 (1973).
- <sup>20</sup>F. Van Steen and D. Schoemaker, *Phys. Rev. B* **19**, 55 (1979).
- <sup>21</sup>E. Goovaerts, S. Nistor, and D. Schoemaker, *Phys. Rev. B* **25**, 83 (1982).
- <sup>22</sup>F. Lüty, in *Physics of Color Centers*, edited by W. B. Fowler (Academic, New York, 1968).
- <sup>23</sup>C. J. Delbecq, R. Hartford, D. Schoemaker, and P. H. Yuster, *Phys. Rev. B* **13**, 3613 (1976).
- <sup>24</sup>D. Schoemaker, *Phys. Rev. B* **3**, 3516 (1971).
- <sup>25</sup>C. J. Delbecq, W. Hayes, and P. H. Yuster, *Phys. Rev.* **121**, 1043 (1961).
- <sup>26</sup>D. Schoemaker and A. Lagendijk, *Phys. Rev. B* **15**, 5927 (1977).
- <sup>27</sup>K. Bachmann and W. Känzig, *Phys. Kondens. Mater.* **7**, 284 (1968).
- <sup>28</sup>D. Schoemaker and E. L. Yasaitis, *Phys. Rev. B* **5**, 4970 (1972).